

New frontiers against antibiotic resistance: A Raman-based approach for rapid detection of bacterial susceptibility and biocide-induced antibiotic cross-tolerance

Original

New frontiers against antibiotic resistance: A Raman-based approach for rapid detection of bacterial susceptibility and biocide-induced antibiotic cross-tolerance / Barzan, Giulia; Sacco, Alessio; Mandrile, Luisa; Giovannozzi, Andrea M.; Brown, James; Portesi, Chiara; Alexander, Morgan R.; Williams, Paul; Hardie, Kim R.; Rossi, Andrea M.. - In: SENSORS AND ACTUATORS. B, CHEMICAL. - ISSN 0925-4005. - ELETTRONICO. - 309:(2020). [10.1016/j.snb.2020.127774]

Availability:

This version is available at: 11583/2786436 since: 2020-01-30T15:23:21Z

Publisher:

Elsevier

Published

DOI:10.1016/j.snb.2020.127774

Terms of use:

This article is made available under terms and conditions as specified in the corresponding bibliographic description in the repository

Publisher copyright

Elsevier postprint/Author's Accepted Manuscript

© 2020. This manuscript version is made available under the CC-BY-NC-ND 4.0 license
<http://creativecommons.org/licenses/by-nc-nd/4.0/>. The final authenticated version is available online at:
<http://dx.doi.org/10.1016/j.snb.2020.127774>

(Article begins on next page)

New frontiers against antibiotic resistance: A Raman-based approach for rapid detection of bacterial susceptibility and biocide- induced antibiotic cross-tolerance

Giulia Barzan^{a,b}, Alessio Sacco^{a,b}, Luisa Mandrile^a, Andrea M.
Giovannozzi^{a*}, James Brown^c, Chiara Portesi^a, Morgan R. Alexander^d,
Paul Williams^c, Kim R. Hardie^c, and Andrea M. Rossi^a

^a *Quantum Metrology and Nano Technologies Division, Istituto Nazionale di Ricerca
Metrologica (INRiM), Strada delle Cacce, 91, 10135 Turin, Italy;*

^b *Department of Electronics and Telecommunications, Politecnico di Torino, Corso Duca
degli Abruzzi, 24, 10129 Turin, Italy;*

^c *School of Life Sciences, Centre for Biomolecular Sciences, University of Nottingham,
Nottingham NG7 2RD, UK;*

^d *School of Pharmacy, University of Nottingham, Nottingham NG7 2RD, UK*

^{*} *Corresponding author: Andrea M. Giovannozzi, tel +39 011 3919330; e-mail*

a.giovannozzi@inrim.it

Abstract

To overcome the widespread misuse of antibiotics and reduce the growing problem of multidrug resistance, rapid, sensitive and specific novel methods to determine bacterial antibiotic susceptibility are needed. This study presents a combined dielectrophoresis (DEP) - Raman Spectroscopy (RS) method to obtain direct, real-time measurements of the susceptibility of a suspension of planktonic bacteria without labelling or other time-consuming and intrusive sample preparation processes. Using an in-house constructed DEP-Raman device, we demonstrated the susceptibility of *Escherichia coli* MG1655 towards the second-generation fluoroquinolone antibiotic ciprofloxacin (CP) after only 1 h of treatment, by monitoring spectral changes in the chemical fingerprint of bacteria related to the mode of action of the drug. Spectral variance was modelled by multivariate techniques and a classification model was calculated to determine bacterial viability in the exponential growth phase at the minimum bactericidal concentration (MBC) over a 3 h time span. Further tests at a sub-minimum inhibitory concentration (MIC) and with a CP-resistant *E. coli* were carried out to validate the model. The method was then successfully applied for class prediction in a biocide cross-induced tolerance assay that involved pre-treating *E. coli* with triclosan (TCS), an antimicrobial used in many consumer products. High specificity and adequate sensitivity of the proposed method was thereby demonstrated. Simultaneously, standard microbiological assays based on cell viability, turbidity and fluorescence microscopy, were carried out as reference methods to confirm the observed Raman response.

Keywords: Raman spectroscopy, dielectrophoresis, E. coli, antibiotic resistance, ciprofloxacin, antibiotic susceptibility test

Introduction

The overuse and misuse of antibiotics has led to the selection of multidrug-resistant organisms (MDROs) such that multi-drug resistance has become a global emergency (WHO, 2014). Moreover, the extensive use of biocides in everyday life has also contributed to an increase in the resistance or tolerance of bacteria to a range of antimicrobial agents (Chapman, 2003). Residues of antimicrobials on surfaces create a chemical reservoir, exposing bacteria colonizing such a niche to sub-lethal concentrations of these agents (Lyman and Furia, 1969). This potential antimicrobial reservoir may persist for a significant amount of time, resulting in prolonged exposure. It is possible that this may induce tolerance or select for resistance in bacteria that subsequently colonize hosts as part of the commensal microbiota or, more worryingly, as pathogens that go on to cause debilitating infections (Jutkina et al., 2018). It has been reported that exposure to one antimicrobial can induce a change in bacterial susceptibility to another, and this will be referred to as "cross-induced tolerance" (Lavilla Lerma et al., 2015).

Within this context, it is clear that there is an urgent need for novel methods to rapidly evaluate the susceptibility of bacteria to specific antibiotics, in order to prescribe effective, tailored therapies, thereby reducing the likelihood of creating an environment that will select for antibiotic resistance (O'Neill, 2015). Many recent studies have focused on overcoming the time-consuming steps used in classical microbiological methods for antibiotic susceptibility testing (AST), such as disc diffusion, gradient diffusion, and agar/broth dilution (Jorgensen and Ferraro, 2002). These methods take time because they require overnight incubation to determine minimum inhibitory concentrations (MICs). The new approaches are mainly based on molecular methods, i.e. polymerase chain reaction (PCR) (Sibley et al., 2012) or mass spectrometry (Lupo et al., 2015), which require expensive reagents or equipment and take a considerable time for sample preparation. Schröder and Kirchhoff demonstrated that,

compared with other spectroscopic methods (Lasch and Naumann, 2015), Raman spectroscopy (RS) has potential for fast bacterial identification and antibiotic susceptibility profiling (Schröder et al., 2015). RS is a label-free, non-contact, culture-independent technique, which does not require any toxic immunochemical staining and benefits from minimal sample preparation time. Furthermore, dielectrophoresis (DEP) can be employed in combination with RS to aggregate bacteria, increasing their local population density and optimizing the Raman signal to noise ratio of dispersed samples (Kirchhoff et al., 2018; Schröder et al., 2013).

Here, a combined DEP-Raman approach was developed to rapidly test bacterial susceptibility to antibiotics, reducing the total time for sample analysis and for the first time predictive models to evaluate bacterial susceptibility in a situation of cross-induced tolerance were employed.

Initially, *Escherichia coli* susceptibility towards the second-generation fluoroquinolone ciprofloxacin (CP) drug (Fasugba et al., 2015) was analysed to obtain a data set for the training of a statistical classification model. CP was used as it is one of the most common antibiotics prescribed to treat UTIs (Urinary Tract Infections) caused by *E. coli* (Lindgren et al., 2003). Furthermore, fluoroquinolone-resistant *E. coli* have been isolated in many different European countries (Cagnacci et al., 2008). Thus, rapid antibiotic susceptibility testing is urgently needed to determine whether fluoroquinolones can be administered to treat *E. coli* UTIs.

Using our in-house constructed DEP-Raman microfluidic device, we were able to perform dynamic measurements of the susceptibility of planktonic bacteria treated with antibiotic without any staining or complex sample preparation. The purpose of this work was to develop a robust classification model, precise and accurate enough to rapidly determine Raman spectral differences between sensitive *E. coli* MG1655 treated with ciprofloxacin and negative controls. These can be used to predict bacterial susceptibility to CP and other antimicrobial

agents. In this study, systematic differences in the RS spectra of bacteria were identified as a function of exposure time, experimental replicates and antibiotic treatment that could be assigned a statistical significance by analysis of variance-simultaneous component analysis (ASCA). The predictive ability and sensitivity of the obtained model was tested twice: by applying it to *E. coli* MG1655 treated with a sub-MIC concentration of CP, and towards an *E. coli* strain resistant to CP (*E. coli* PSA-I). In both cases, a good accuracy of classification of the model was demonstrated. Furthermore, we applied the model in an experimental system in which tolerance to CP was induced by the pre-treatment of *E. coli* MG1655 with a sub-MIC concentration of triclosan, a biocide present in many consumer products (toothpaste, soaps, detergents, toys etc.), that drives selection for multi-drug resistance (MDR) (Carey and McNamara, 2014).

Materials and Methods

Reagents

TCS and CP were purchased from Sigma-Aldrich. Stock solutions were prepared in HCl 0.1 M for CP while TCS was dissolved in ethanol. Subsequently, dilutions in Milli-Q water were prepared for both drugs to obtain the correct concentrations adopted for the AST and the induced tolerance assay.

LB broth, agar and PBS tablets pH 7.4 (for 200 ml) were purchased from Sigma-Aldrich and diluted in Milli-Q water and autoclaved for 20 min at 121 °C.

Fluorescent dyes DAPI (ThermoFisher Scientific, D1306) and FM5-95 (ThermoFisher Scientific, T23360) were prepared in PBS for use in the fluorescent imaging of the bacteria.

Bacterial strains and cultivation

E. coli MG1655, a CP susceptible laboratory strain, *P. aeruginosa* PAO1 (Nottingham sub-line), *Staphylococcus aureus* SH1000 (University of Nottingham strain collection) and *E. coli*

PSA-I, a CP resistant environmental isolate strain (obtained from Matthew Avison; University of Bristol, UK) were cultivated and prepared for Raman analysis as specified in the Supplementary information (SI).

The MIC (minimum inhibitory concentration) and MBC (minimum bactericidal concentration) of CP against *E. coli* MG1655 were determined as specified in the SI.

Morphological analysis by fluorescence microscopy

Bacterial membranes were stained by addition of 2 μ l FM5-95 (Sigma-Aldrich; 200 μ g/ml) to 30 μ l culture; DNA in the nucleoids was stained by addition of 1 μ l DAPI solution (1 mg/ml) to 6 μ l of the culture prior to mounting on a microscope slide coated with a thin film of 1.2% agarose.

Images were acquired using a Nikon Digital Sight DS-Fi1 camera attached to a Nikon Eclipse 50i microscope equipped with an Intensilight C-HGFI light source.

Bacterial characterization by the DEP-Raman device

A drop of bacterial suspension (\sim 100 μ l) was injected into the Raman-DEP microfluidic device and Raman spectra collected in the centre of the cell. The procedure for device set-up is reported in SI. The optimal electrical field in the DEP cell for *E. coli* was a sinusoidal voltage of 5 V peak to peak at a frequency of 1 MHz; the bacterial accumulation time before acquisition was 6 min.

The samples were analysed with a DXR™ Raman confocal microscope (Thermo Scientific). Each spectrum was acquired using an excitation wavelength at 532 nm, a laser power of 10 mW with an exposure time of 2.5 s for 24 scans (1 min per spectrum) and a spectrograph confocal pinhole aperture of 50 μ m in diameter. Spectra were collected with the dispersive Raman system with a 5 cm^{-1} spectral resolution and a spectral range of 3100–500 cm^{-1} with

3489 points per spectrum. The objective employed in this study was a 60× water immersion with a numerical aperture of 1.1.

Data analysis and multivariate modelling

PLS Toolbox (Eigenvector Research, Inc., Manson, WA) for Matlab R2015a (Mathworks, Natick, MA) was used for chemometric analysis. Spectra were pre-processed by Savitsky-Golay smoothing (window width 35 points, polynomial order 2), baseline correction by weighted least squares (polynomial order 2), mean centring and intensity normalization on the CH_x vibrational modes at 2940 cm⁻¹ to eliminate the possible spectral differences due to a variation of the number of bacterial cells aggregated under the spot of the laser. Analysis of variance-simultaneous component analysis (ASCA) was used to determine the effect of different experimental parameters (Smilde et al., 2005). The factors considered were (i) “time”, 1 h, 2 h, and 3 h; (ii) “drug”, untreated (class 0, control) or treated (class 1, test); (iii) “experiment”, the different cell culture batches. 2-way correlations between factors were considered. The significance was determined by p-values through permutation tests by randomizing the levels belonging to the factor under consideration within the levels of each other factor (Zwanenburg et al., 2011, Mandrile et al., 2019). The H₀ hypothesis of no experimental effect, with a confidence level of p was tested.

PLS-DA classification models were built by a training set of independent experiments conducted at different times and validated by predicting independent spectra acquired from new experiments. We calculated the following figures of merit: sensitivity [true positive/(true positive+false negative)], specificity [true negative/(true negative+false positive)], and classification error (1-accuracy) where accuracy is the ratio (correctly classified samples)/(total samples as classification).

Results and discussion

Bacterial characterization by Raman

The combined DEP-Raman technique was applied to test the susceptibility of *E. coli* MG1655 to the commonly prescribed second-generation fluoroquinolone antibiotic, ciprofloxacin, by monitoring spectral changes in the chemical fingerprint of the bacteria. Molecules predicted to be modulated as a result of the mode of action of the drug were specifically monitored. The integrated dielectrophoresis-Raman setup and the cell fabrication process (fig. 1a) are described in detail in SI. After bacterial accumulation in the centre of the DEP cell, Raman spectra were acquired using a water immersion objective (fig. 1b).

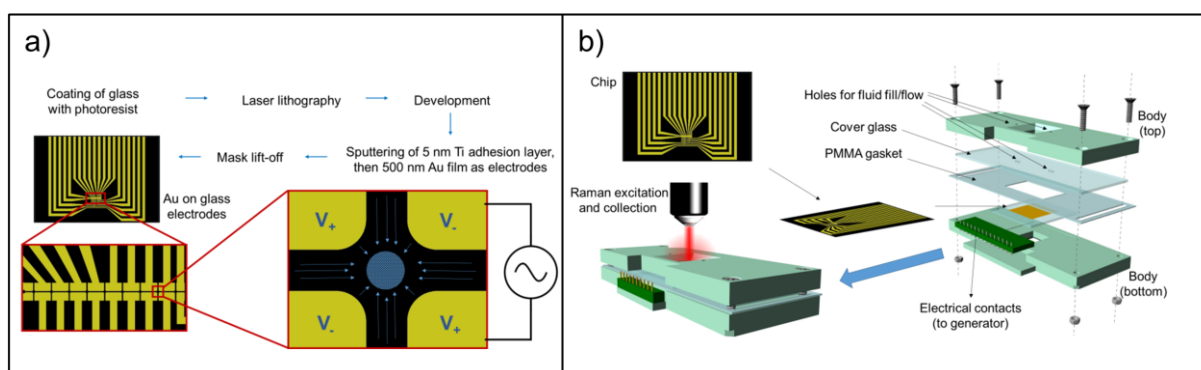


Figure 1: DEP cell fabrication.

a) Scheme of active chip preparation and positioning within the sample holder. The electric field is generated when voltage is applied: bacterial cells accumulate in the centre of the four electrodes pushed by DEP forces (blue arrows). The distance between the tips of the two electrodes of the same polarity (V_+ , V_+) in the DEP cell is 40 μm , while the gap between the two electrodes of opposite polarity (V_+ , V_-) is 20 μm . b) Schematic representation of the sample holder. Bacteria dispersed in liquid medium are injected into the holes near the window, the voltage applied, and the laser beam focussed into the centre of the window.

Optimising the conditions of spectra collection for *E. coli* MG1655, such as voltage and frequency, a satisfactory signal to noise ratio was obtained, which allowed us to characterize the strain and assign a chemical functional group to each typical bacterial Raman band within

the different regions of the chemical fingerprint (SI fig.S1 and table S1). The versatility of our DEP-Raman setup was also successfully demonstrated to the characterization of two other bacterial strains, one Gram positive (*S. aureus* SH1000), and one Gram negative (*P. aeruginosa* PAO1) (SI fig. S2). The MIC and MBC of ciprofloxacin against *E. coli* MG1655 were determined to be 0.5 µg/ml and 1 µg/ml respectively to benchmark this particular strain for use as a basis for the design of the subsequent experiments (SI fig. S3a and S3b). A seed culture at OD₆₀₀ (optical density at 600 nm) of 0.3 was chosen to inoculate cultures so that the bacteria would be in mid-exponential growth phase. At this point, bacteria are growing exponentially, a phase of growth where they are rapidly multiplying and are more sensitive to antibiotics such that there is a higher chance that mutations conferring resistance against antimicrobials will arise (Kloß et al., 2013). Raman analyses of *E. coli* MG1655 were performed using the DEP-Raman setup described in the previous paragraph. Comparisons were made between untreated bacterial cultures and parallel bacterial cultures treated with CP at 1 µg/ml for four different time periods (0 h, 1 h, 2 h and 3 h).

The collection volume of the Raman microscope in the conditions employed in this work is 4.7 µm³. On the basis of the optical microscopy images of *E. coli* MG1655 untreated cells obtained it was calculated that no more than 6–10 cells were investigated during Raman measurements (ciprofloxacin-affected bacteria have higher, variable volumes, so in these cases the number was smaller).

Simultaneously, standard microbiological assays based on cell viability, culture turbidity and fluorescence microscopy were undertaken. The data generated served as reference methods to correlate the observations from Raman analysis (fig. 2).

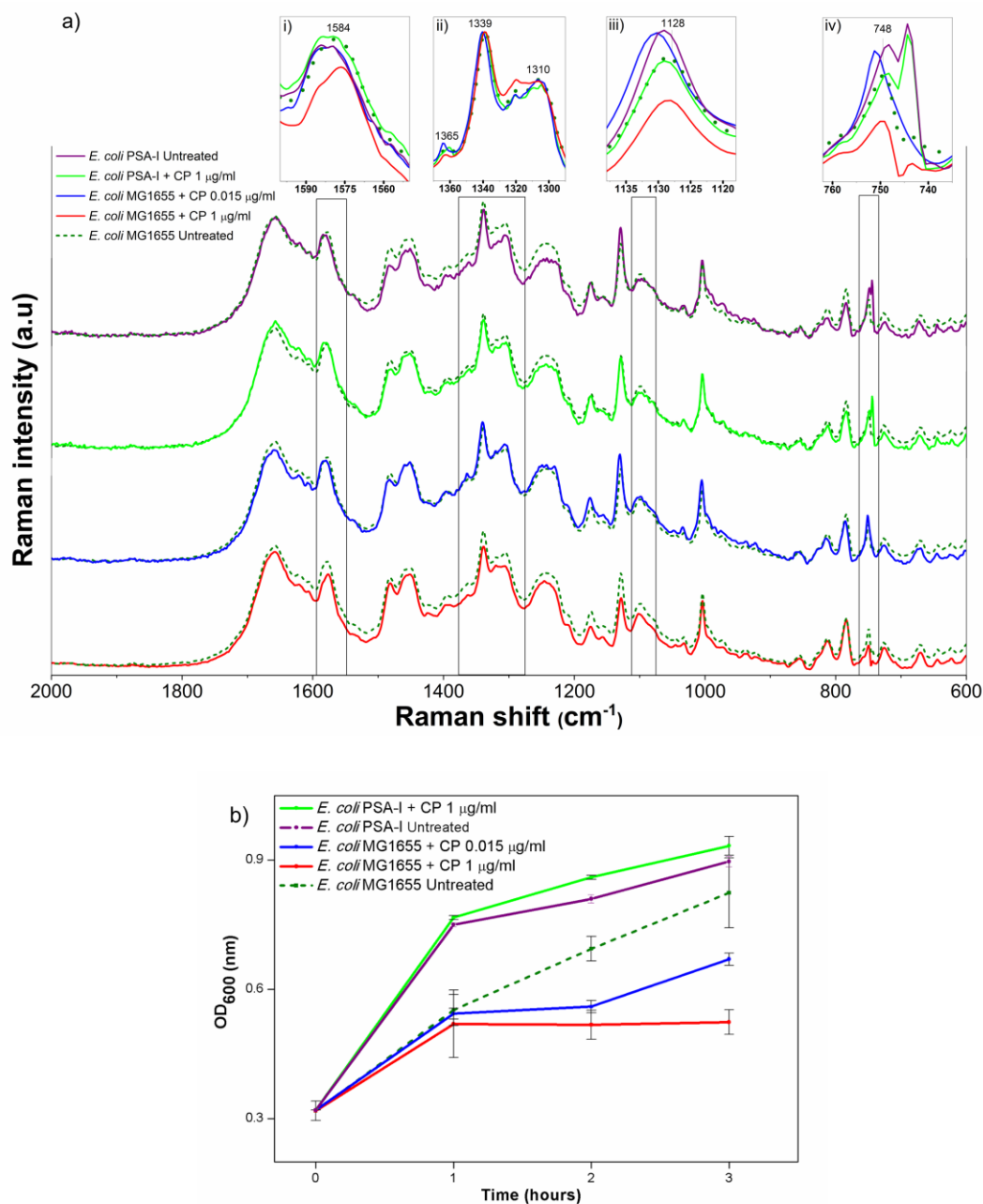


Figure 2: Biological and DEP-Raman analysis of *E. coli* in the presence and absence of a range of concentrations of CP over a 3 h period.

a) DEP-Raman spectra of *E. coli* MG1655 untreated (dash olive), treated with CP at the MBC (red), with CP at sub-MIC levels (0.015 µg/ml) (blue), *E. coli* PSA-I untreated (purple) and *E. coli* PSA-I treated with CP at the MBC for 1h (green). Inserts: spectral regions of interest that exhibit the most evident differences. For insert ii): spectra were normalized against the peak at 1339 cm⁻¹ (tryptophan vibrational modes). b) Optical density (turbidity) assay of *E. coli* strains MG1655 and PSA-I showing the extent of growth using the same treatments and colour coding as described for panel a. The OD₆₀₀ of the cultures is plotted against incubation time.

The turbidity assay (fig. 2b) verified that bacterial cells treated with CP at the MBC stopped growing after 1 h, because the machinery for DNA replication was stalled by CP-mediated DNA gyrase/topoisomerase inhibition. In support of this, CFU enumeration after exposure to CP for 24 h, resulted in a 99.9% reduction in viability compared with the control (SI fig. S3b). For this reason, we refer to bacterial cells treated with CP at MBC as non-viable, while the untreated cells (control) are considered as viable.

Multivariate data analysis and construction of the classification model

Changes in the spectral profiles of treated and untreated samples were highlighted by explorative principal component analysis (PCA) (see SI fig. S4).

PCA revealed that Raman spectra showed changes related to the antibiotic treatment after only 1 h of antibiotic treatment (see SI fig. S4a) as well as to growth over time (see SI fig. S4b), but notably different spectral regions were represented in the PCs modulated by time or antibiotic treatment (see SI fig. S4c). The signals that varied the most after the antibiotic treatment were those corresponding to the vibrational modes of nucleic acids (fig. 2), which is reasonable since ciprofloxacin targets DNA replication. In particular, we found spectral changes in the band at 1584 cm^{-1} that correspond to the $\nu_{\text{C-N}}$, $\delta_{\text{N-H}}$ of guanine and adenine (Pätzold et al., 2008); in the peak at $748\text{--}750\text{ cm}^{-1}$ corresponding to $\nu_{\text{O-P-O}}$ and aromatic ring vibration of nucleic acids (Movasaghi et al., 2007); and in the spectral region between $1300\text{--}1370\text{ cm}^{-1}$ due to deformation of adenine and guanine ($1302\text{--}1315\text{ cm}^{-1}$) (Deng et al., 1999), tryptophan (1339 cm^{-1}), CH_2/CH_3 twisting, wagging, bending modes of lipids ($1313\text{--}1307\text{ cm}^{-1}$) (Movasaghi et al., 2007) and cytosine (1362 cm^{-1}) (De Gelder et al., 2007).

On the other hand, spectral regions affected by the duration of treatment were more related to protein and lipids. Specifically, there were differences in the region around 1100 cm^{-1} which is related to $\nu_{\text{C-N}}$ and other ring breathing modes of phenylalanine (Phe); in the band at 1240 cm^{-1} which refers to amide III and asymmetric $\nu_{\text{PO}_2^-}$ of DNA bases; in the region between

1338–1310 cm^{-1} corresponding to δ_{CH_2} of tryptophan (Trp), CH bending modes of lipids and ring vibration of guanine and adenine; and in the peak at 1480 cm^{-1} related to CH_2 stretching modes of lipids. In particular, the band at 1240 cm^{-1} was modulated more by the duration of the incubation, than by the presence or absence of antibiotic treatment, which is in accordance with the literature (Schröder et al., 2015). (see SI fig. S4 and S5)

Next, we performed ASCA to evaluate the statistical significance of the differences observed by PCA. ASCA is specifically suited for time-resolved multigroup (viable and inhibited *E. coli*, treated for 1 h, 2 h or 3 h), multi-subject (containing data of multiple culture batches) and multivariate data (such as Raman spectra). The model revealed that both the effect of time (bacterial growth) and of antibiotic treatment trigger significant chemical variations, as does experimental replication. The effects of the different experimental design factors (“time”, “drug” and “experiment”) were separated by the ASCA model and quantified. The factor “time” is predominant over the factor “drug” with effect = 12.56% of variance and $p = 0.001$; the factor “drug” has an estimated effect of 11.73% and $p = 0.001$. Interestingly, the factor “experiment” produced a significant effect (16.27% of variance with $p = 0.001$). In addition, the interaction term of “time \times drug” is significant, which means that the effect of the antibiotic was not constant over time, since the cells responded differently to the drug over a period of 3 h. The scores plot of the PCA models built for the two most interesting effects (“time” and “drug”) shows separation between the groups (fig. 3 a-b) and the loading profiles of PC1 for these two factors reveal the different contribution of original spectral bands in the separation (fig. 3c). This statistically significant separation of groups indicates that the impact of bacterial physiology and growth cannot be neglected and that the drug effect can be successfully detected by Raman spectroscopy. This analysis formed the basis for the construction of predictive classification models.

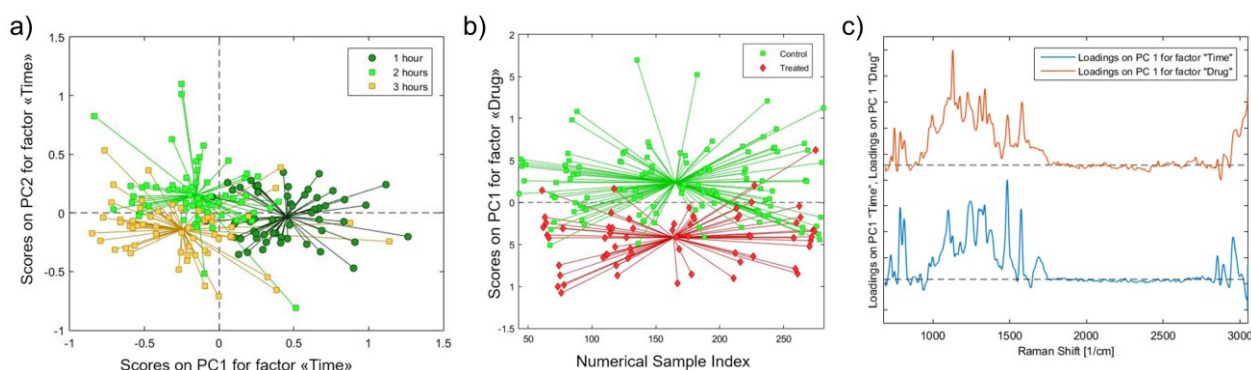


Figure 3: ASCA scores plot considering the first two PCs for the relevant experimental factors.

a) ASCA score plot with respect to factor “time” b) ASCA score plot with respect to factor “drug”. c) Loading profile of PC1 for factors “Time” and “Drug”.

PLS-DA classification models were developed in order to obtain a predictive method for identifying the responses of the cells to antibiotic treatment. One model for each time point was generated, since the time of analysis causes non-negligible changes in the spectra of both treated and controls. Samples treated with CP at the MBC were considered as “non-viable/inhibited” (positive: class 1) and the untreated samples as “viable” (negative: class 0). The sensitivity, specificity and classification errors were calculated (Table 1) and, after only 1 h, good discrimination between the two classes was achieved. From this classification, the susceptibility to antibiotic increases over time, as after 2 h and 3 h, all treated samples were classified as non-viable (no false negatives were registered). Conversely, the specificity of the prediction was highest after only 1 h, because the effect of “time” adds up to that of “treatment”, resulting in a higher number of false positives, i.e. erroneously classified as non-viable. In general, since the total error rate increases over time, we focussed on 1 h experiment where the lowest classification error was achieved. In an AST for investigating antibiotic tolerance, the probability of missing a tolerant culture is considered more serious than overestimating the false negatives (i.e. erroneously classified as viable), so high specificity is required. Furthermore, RS results were more sensitive when compared with

classical microbiological techniques. In fact, major differences between the spectra of treated and untreated samples were already visible after 1 h, while in the turbidity assay, at the same time point, the growth curves almost overlap (fig. 2b).

Table 1: Table of susceptibility, specificity and classification error for PLS-DA models constructed for each time point.

Validation	1 h (%)	2 h (%)	3 h (%)
Sensitivity (Prediction)	67	100	100
Specificity (Prediction)	100	50	33
Classification Error (Prediction)	17	25	33

Validations of the model: E. coli treated with a sub-MIC concentration of CP and E. coli resistant to CP

The predictive strength of our statistical model was tested by performing the same experiment with two concentrations of CP: 0.5 µg/ml (MIC for *E. coli* MG1655 at OD₆₀₀=0.3) and 0.015 µg/ml (sub-MIC).

As CP is an antibiotic that inhibits DNA gyrase and topoisomerase IV (enzymes involved in transcription and DNA replication), thereby blocking bacterial cell division (Fisher et al., 1989), growth (measured as OD₆₀₀) at the MIC concentration shows that bacteria stop replicating after 1 h of treatment (the time necessary for at least two complete cycles of bacterial replication and for the drug to impact on the total cell population). On the other hand, bacteria treated with a sub-MIC of 0.015 µg/ml continue to grow, although at this concentration, growth is slower than that exhibited by the untreated controls (fig 2b).

In agreement with the biological response, the PLS-DA model classified the spectra obtained from *E. coli* treated at MIC as positive (non-viable/inhibited) for CP treatment with an accuracy of 83%. In addition, 83% of bacteria treated at sub-MICs were classified as negative (viable) (SI fig. S6a). In support of this classification, a viable count (CFU) assay was carried

out to determine the MBC. This returned a significant reduction in viable cell numbers after 24 h treatment with 0.5 $\mu\text{g/ml}$ of CP, whereas with 0.015 $\mu\text{g/ml}$ of CP there was no significant difference from the untreated controls (SI fig. S3b). This demonstrates that RS can be used to test the viability of bacteria with adequate accuracy after only 1 h of treatment at different CP concentration levels, in agreement with previous literature (Kirchhoff et al., 2018). Interestingly, the spectral bands varying the most with CP concentration are the same as those that were revealed to be related to the effect of the antibiotic. See ASCA model reported in SI (SI fig S8).

To further confirm the statistical validity of the proposed DEP-Raman method, we applied it to the classification of *E. coli* PSA-I, (a CP resistant environmental isolate morphologically similar to MG1655 (Smart et al., 2019)) untreated and after treatment with CP at the MBC concentration (1 $\mu\text{g/ml}$).

As the turbidity assay in Fig. 2b clearly shows, *E. coli* PSA-I was not inhibited by treatment with CP at the MBC, but continued to grow at the same rate as the untreated *E. coli* PSA-I strain. In accordance with the microbiological results, the Raman spectra profile of *E. coli* PSA-I + CP 1 $\mu\text{g/ml}$ (green line) highlight more similarities with *E. coli* MG1655 untreated control (olive dash line) than with the treated MG1655 sample (red line) (fig. 2). The model correctly assigned 100% of *E. coli* PSA-I Raman spectra to the class of negative bacteria (viable) after only 1 h of CP treatment (SI fig. S6b) and correctly classified 89% of the PSA-I untreated samples. This test is relevant because attests the versatility of the model also testing different bacterial strains, even though they slightly differ from the training set (see SI for further details, fig. S7). The robustness of the model was confirmed since the scores of resistant *E. coli* were positioned below the discriminant line, nearer to negative cells (viable). Furthermore, this experiment confirmed the applicability of the model to predict the susceptibility of the bacteria to a specific antibiotic.

Application of the model to biocide cross-induced tolerance

Triclosan (TCS), one of the most widely used antimicrobial agents for personal hygiene purposes, has previously been shown to induce cross-tolerance to antibiotics in different bacterial species. This tolerance can be induced at TCS concentrations lower than 1 µg/ml (Carey and McNamara, 2014), which is far below the MIC for most bacterial strains as well as at concentrations commonly found in the environment. As demonstrated by Westfall et al, (Westfall et al., 2019), TCS has a dramatic protective effect on *E. coli*, increasing its survival in the presence of ciprofloxacin (100 ng/ml: $\sim 3\times$ MIC) in *in vitro* experiments as well as *in vivo*, in murine infection models. In order to induce antibiotic tolerance, *E. coli* was pre-treated with a TCS concentration found in the urine of individuals using triclosan-containing products (0.2 µg/ml) (Calafat et al., 2008; MacIsaac et al., 2014). Thereafter, we tested the susceptibility of our DEP-RS method to detect cross-induced tolerance to ciprofloxacin in *E. coli* MG1655.

Fluorescence microscopy and viable count (CFU) assays (SI fig.S6) were performed on bacterial samples for each treatment to support the Raman results at the biological level using established microbiological methods.

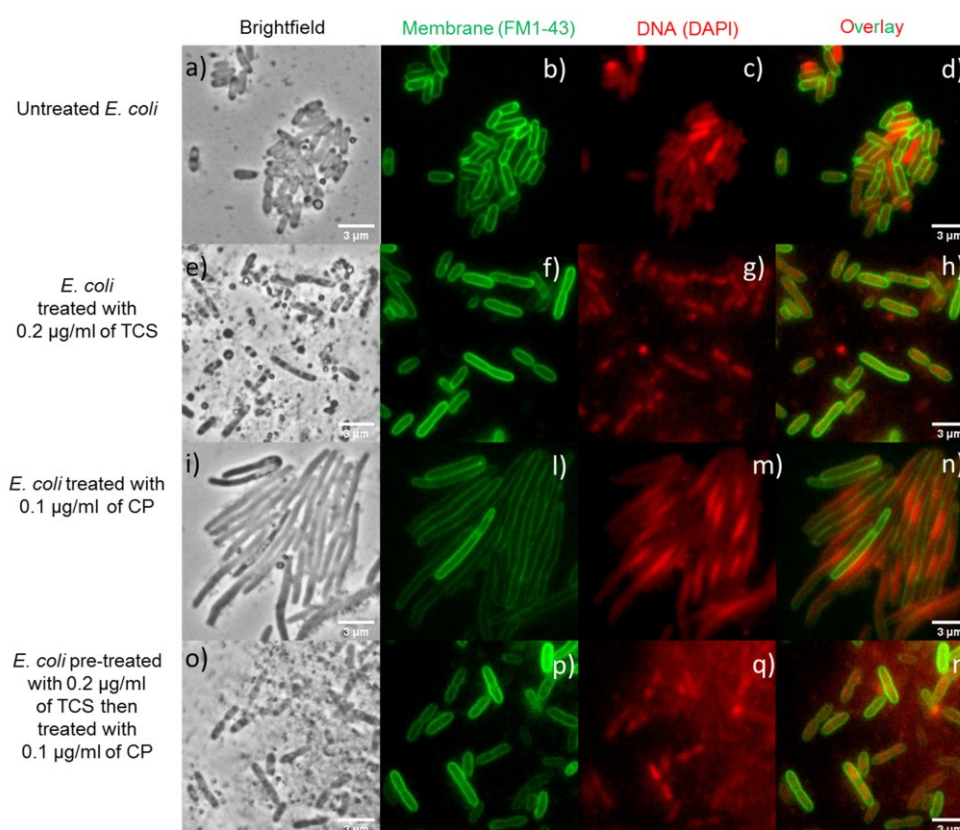


Figure 4: Fluorescence microscopy of *E. coli* MG1655 treated with or without 0.5 µg/ml of ciprofloxacin or 0.2 µg/ml of triclosan or treated with both drugs for 1 h.

Untreated (a–d) or bacteria treated with TCS (e–h), CP (i–n) or both TCS and CP (o–r) are shown in bright field (a,e,i,o), stained for bacterial membranes (b,f,l,p; green), for DNA (c,g,m,q; red) or with membrane and DNA stains overlaid (d,h,n,r).

As fig. 4 shows, CP induces filamentation in *E. coli* MG1655 after only 1 h of treatment at the MIC (0.5 µg/ml). In particular, filamentation together with changes in DNA localization is evident in bacteria treated with CP (fig. 4 l,m,n) compared with the controls (fig. 4 a–d). This is consistent with a blockage in cell division and induction of the SOS DNA repair response, as would be expected from the mechanism of action of CP. Interestingly, in the bacterial samples treated for 1 h with both compounds, the typical morphology of untreated bacterial cells is retained in terms of both cell shape and DNA localization (fig. 4 p–r). This supports the gain of tolerance to CP, because the cells were able to divide again when pre-treated with TCS even in presence of CP at the MIC.

Fluorescence microscopy demonstrated that 1 h of treatment with ciprofloxacin at the MIC is enough to observe the effects of the antibiotic on cell morphology and intracellular DNA distribution. Furthermore, it shows that bacteria pre-treated with TCS are able to develop a cross-tolerance to CP after just 1 h of exposure.

The same samples were also analysed by DEP-RS device and the spectra were classified with the PLS-DA model that was previously validated.

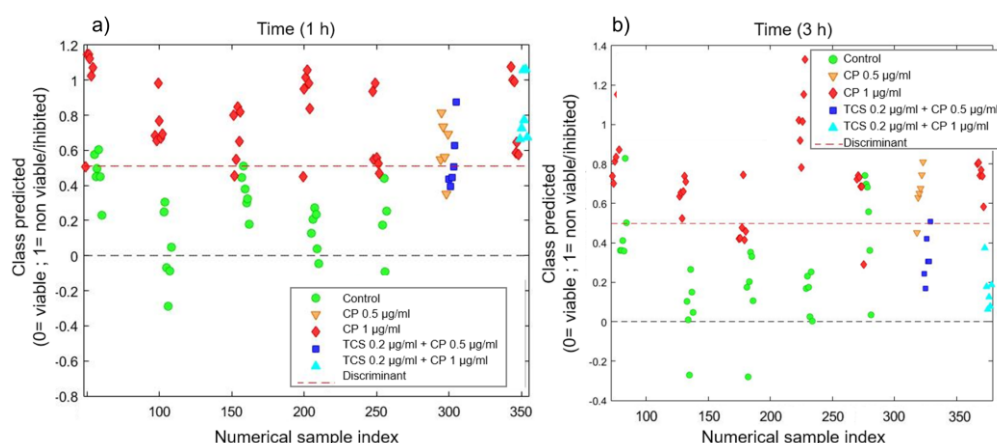


Figure 5: PLS-DA prediction plots for *E. coli* MG1655 treated with TCS and CP. Classification of *E. coli* MG1655 pre-treated with TCS then treated with CP at MIC (dark blue squares) or MBC (light blue triangles) and controls treated only with CP at MIC (yellow triangles) or MBC (red diamonds). The training set data are also reported as green circles and red diamonds for “viable” and “non-viable/inhibited” bacteria, respectively. a) Classification after treatment for 1 h with CP. b) Classification after a treatment for 3 h with CP.

Fig. 5 demonstrates that most of bacteria treated with CP at the MIC (yellow triangles) were classified as non-viable/inhibited (which serves as a control test in this experiment, and are considered the negatives for the calculation of sensitivity and specificity, in this case). Bacteria treated with both drugs were successfully classified as tolerant. The sensitivity of the classification is 66% after 1 h of treatment (fig. 5a) and rises to 83% after 3 h (fig. 5b). This confirmed that DEP-RS approach is able to reveal the gain in cross-induced tolerance after only 1 h of TCS treatment, in accordance with the results obtained with biological assays. Moreover, the induced tolerance was detected more sensitively after prolonged CP treatment.

This could be explained as the greater adaptability of bacterial cells to CP after 3 h, clearly showing the induced tolerance provided by the TCS pre-treatment. The same experiment of cross-induced tolerance was performed with a CP concentration corresponding to the MBC. The effect on *E. coli* cells was evaluated using the validated DEP-RS method. In this case we noticed that 1 h of treatment is not enough to observe the induced tolerance effect but this appears after 3 h (sensitivity 100%), confirming that prolonged experiments permit detection of cross-induced tolerance also at higher CP concentrations, i.e. at the MBC.

Conclusions

Developing a new rapid AST that would give a response in a few hours instead of a few days is a key challenge in clinical and microbiological fields. Saving time is essential not only to promote optimal patient outcomes, but also to prevent or reduce selection for antibiotic-resistant organisms (Laxminarayan et al., 2013).

The DEP-Raman device developed here allows characterization of different bacterial strains with high specificity and to follow dynamic interactions of the bacteria with antibiotics.

Raman results processed with multivariate data analysis are able to model spectral differences at a molecular level between treated or untreated bacterial cells after only 1 h of treatment.

The susceptibility test based on Raman allowed us to correctly classify as non-susceptible bacteria treated with a sub-MIC concentration of CP and bacteria in which tolerance to the antibiotic was induced by TCS pre-treatment. An environmental *E. coli* strain naturally resistant to CP (PSA-I) was also successfully predicted as non-susceptible after 1 h of treatment with CP at MBC.

The combined DEP-Raman results obtained were confirmed by standard microbiological assays that revealed that the induced tolerance was significant at all three time points after treatment. The proposed combined DEP-Raman method could open the way to a new rapid bacterial antibiotic susceptibility test, without the necessity of time-consuming sample

preparation and the overnight incubation required by classical microbiological techniques, with high accuracy and versatility for several applications.

Acknowledgements

The present work has been supported by the project “15HLT01 MetVsBadBugs” which has received funding from the EMPIR programme co-financed by the Participating States and from the European Union's Horizon 2020 research and innovation programme.

Part of this work was carried out in collaboration with the Centre for Biomolecular Science of Nottingham University (UK). We thank Dean Walsh for his advice about TCS experiments.

We thank Matthew Avison (University of Bristol) for sharing the strain PSA-1.

Notes

The authors declare no competing financial interest.

Supplementary Information

Bacterial cultivation and exposure to antimicrobials methods; Design and fabrication of the DEP cell details; Raman-DEP characterization of *E. coli* MG1655, *S. aureus* SH1000 and *P. aeruginosa* PAO1 (spectra and band assignments); Determination of MIC and MBC of CP towards *E. coli* MG1655 at OD600 0.3; Supplementary information on data analysis, multivariate modelling and validation; Biological evidence of triclosan-ciprofloxacin cross-induced tolerance.

References

- Cagnacci, S., Gualco, L., Debbia, E., Schito, G.C., Marchese, A., 2008. European emergence of ciprofloxacin-resistant *Escherichia coli* clonal groups O25:H4-ST 131 and O15:K52:H1 causing community-acquired uncomplicated cystitis. *J. Clin. Microbiol.* 46, 2605–2612. <https://doi.org/10.1128/JCM.00640-08>
- Calafat, A.M., Ye, X., Wong, L.Y., Reidy, J.A., Needham, L.L., 2008. Urinary concentrations of triclosan in the U.S. population: 2003-2004. *Environ. Health Perspect.* <https://doi.org/10.1289/ehp.10768>
- Carey, D.E., McNamara, P.J., 2014. The impact of triclosan on the spread of antibiotic resistance in the environment. *Front. Microbiol.* 5, 1–11. <https://doi.org/10.3389/fmicb.2014.00780>
- Chapman, J.S., 2003. Disinfectant resistance mechanisms, cross-resistance, and co-resistance, in: *International Biodeterioration and Biodegradation*. pp. 271–276. [https://doi.org/10.1016/S0964-8305\(03\)00044-1](https://doi.org/10.1016/S0964-8305(03)00044-1)
- De Gelder, J., De Gussem, K., Vandenabeele, P., Moens, L., 2007. Reference database of Raman spectra of biological molecules. *J. Raman Spectrosc.* <https://doi.org/10.1002/jrs.1734>
- Deng, H., Bloomfield, V.A., Benevides, J.M., Thomas, G.J., 1999. Dependence of the raman signature of genomic B-DNA on nucleotide base sequence. *Biopolymers* 50, 656–666. [https://doi.org/10.1002/\(SICI\)1097-0282\(199911\)50:6<656::AID-BIP10>3.0.CO;2-9](https://doi.org/10.1002/(SICI)1097-0282(199911)50:6<656::AID-BIP10>3.0.CO;2-9)
- Fasugba, O., Gardner, A., Mitchell, B.G., Mnatzaganian, G., 2015. Ciprofloxacin resistance in community- and hospital-acquired *Escherichia coli* urinary tract infections: A systematic review and meta-analysis of observational studies. *BMC Infect. Dis.* <https://doi.org/10.1186/s12879-015-1282-4>

- Fisher, L.M., Lawrence, J.M., Josty, I.C., Hopewell, R., Margerrison, E.E.C., Cullen, M.E., 1989. Ciprofloxacin and the fluoroquinolones. New concepts on the mechanism of action and resistance. *Am. J. Med.* [https://doi.org/10.1016/0002-9343\(89\)90010-7](https://doi.org/10.1016/0002-9343(89)90010-7)
- Jorgensen, J.H., Ferraro, M.J., 2002. Antimicrobial Susceptibility Testing: Special Needs for Fastidious Organisms and Difficult-to-Detect Resistance Mechanisms. *Clin. Infect. Dis.* 30, 799–808. <https://doi.org/10.1086/313788>
- Jutkina, J., Marathe, N.P., Flach, C.F., Larsson, D.G.J., 2018. Antibiotics and common antibacterial biocides stimulate horizontal transfer of resistance at low concentrations. *Sci. Total Environ.* 616–617, 172–178. <https://doi.org/10.1016/j.scitotenv.2017.10.312>
- Kirchhoff, J., Glaser, U., Bohnert, J.A., Pletz, M.W., Popp, J., Neugebauer, U., 2018. Simple Ciprofloxacin Resistance Test and Determination of Minimal Inhibitory Concentration within 2 h Using Raman Spectroscopy. *Anal. Chem.* 90, 1811–1818. <https://doi.org/10.1021/acs.analchem.7b03800>
- Lasch, P., Naumann, D., 2015. Infrared Spectroscopy in Microbiology, in: *Encyclopedia of Analytical Chemistry*. <https://doi.org/10.1002/9780470027318.a0117.pub2>
- Lavilla Lerma, L., Benomar, N., Casado Muñoz, M. del C., Gálvez, A., Abriouel, H., 2015. Correlation between antibiotic and biocide resistance in mesophilic and psychrotrophic *Pseudomonas* spp. isolated from slaughterhouse surfaces throughout meat chain production. *Food Microbiol.* <https://doi.org/10.1016/j.fm.2015.04.010>
- Laxminarayan, R., Duse, A., Wattal, C., Zaidi, A.K.M., Wertheim, H.F.L., Sumpradit, N., Vlieghe, E., Hara, G.L., Gould, I.M., Goossens, H., Greko, C., So, A.D., Bigdeli, M., Tomson, G., Woodhouse, W., Ombaka, E., Peralta, A.Q., Qamar, F.N., Mir, F., Kariuki, S., Bhutta, Z.A., Coates, A., Bergstrom, R., Wright, G.D., Brown, E.D., Cars, O., 2013. Antibiotic resistance-the need for global solutions. *Lancet Infect. Dis.*

[https://doi.org/10.1016/S1473-3099\(13\)70318-9](https://doi.org/10.1016/S1473-3099(13)70318-9)

Lindgren, P.K., Karlsson, Å., Hughes, D., 2003. Mutation rate and evolution of fluoroquinolone resistance in *Escherichia coli* isolates from patients with urinary tract infections. *Antimicrob. Agents Chemother.* 47, 3222–3232.
<https://doi.org/10.1128/AAC.47.10.3222-3232.2003>

Lupo, A., Papp-Wallace, K.M., Bonomo, R.A., Endimiani, A., 2015. Non-Phenotypic Tests to Detect and Characterize Antibiotic Resistance Mechanisms in Enterobacteriaceae, in: *Antimicrobial Resistance and Food Safety: Methods and Techniques*.
<https://doi.org/10.1016/B978-0-12-801214-7.00012-0>

Lyman, F.L., Furia, T., 1969. Toxicology of 2, 4, 4'-trichloro-2'-hydroxy-diphenyl ether. *IMS. Ind. Med. Surg.* 38, 64–71.

MacIsaac, J.K., Gerona, R.R., Blanc, P.D., Apatira, L., Friesen, M.W., Coppolino, M., Janssen, S., 2014. Health care worker exposures to the antibacterial agent triclosan. *J. Occup. Environ. Med.* <https://doi.org/10.1097/JOM.0000000000000183>

Mandrile, L., Rotunno, S., Miozzi, L., Vaira, A.M., Giovannozzi, A.M., Rossi, A.M., Noris, E., 2019. Nondestructive Raman Spectroscopy as a Tool for Early Detection and Discrimination of the Infection of Tomato Plants by Two Economically Important Viruses. *Anal. Chem.* <https://doi.org/10.1021/acs.analchem.9b01323>

Movasaghi, Z., Rehman, S., Rehman, I.U., 2007. Raman spectroscopy of biological tissues. *Appl. Spectrosc. Rev.* 42, 493–541. <https://doi.org/10.1080/05704920701551530>

O'Neill, J., 2015. Rapid Diagnostics: Stopping Unnecessary Use of Antibiotics. *Rev. Antimicrob. Resist.* 1–36.

Pätzold, R., Keuntje, M., Theophile, K., Müller, J., Mielcarek, E., Ngezahayo, A., Anders-von

- Ahlften, A., 2008. In situ mapping of nitrifiers and anammox bacteria in microbial aggregates by means of confocal resonance Raman microscopy. *J. Microbiol. Methods* 72, 241–248. <https://doi.org/10.1016/j.mimet.2007.12.003>
- Schröder, U.C., Beleites, C., Assmann, C., Glaser, U., Hübner, U., Pfister, W., Fritzsche, W., Popp, J., Neugebauer, U., 2015. Detection of vancomycin resistances in enterococci within 3 1/2; Hours. *Sci. Rep.* 5, 1–7. <https://doi.org/10.1038/srep08217>
- Schröder, U.C., Ramoji, A., Glaser, U., Sachse, S., Leiterer, C., Csaki, A., Hübner, U., Fritzsche, W., Pfister, W., Bauer, M., Popp, J., Neugebauer, U., 2013. Combined dielectrophoresis-Raman setup for the classification of pathogens recovered from the urinary tract. *Anal. Chem.* 85, 10717–10724. <https://doi.org/10.1021/ac4021616>
- Sibley, C.D., Peirano, G., Church, D.L., 2012. Molecular methods for pathogen and microbial community detection and characterization: Current and potential application in diagnostic microbiology. *Infect. Genet. Evol.* <https://doi.org/10.1016/j.meegid.2012.01.011>
- Smart, A., de Lacy Costello, B., White, P., Avison, M., Batty, C., Turner, C., Persad, R., Ratcliffe, N., 2019. Sniffing out resistance – Rapid identification of urinary tract infection-causing bacteria and their antibiotic susceptibility using volatile metabolite profiles. *J. Pharm. Biomed. Anal.* <https://doi.org/10.1016/j.jpba.2019.01.044>
- Smilde, A.K., Jansen, J.J., Hoefsloot, H.C.J., Lamers, R.J.A.N., van der Greef, J., Timmerman, M.E., 2005. ANOVA-simultaneous component analysis (ASCA): A new tool for analyzing designed metabolomics data. *Bioinformatics* 21, 3043–3048. <https://doi.org/10.1093/bioinformatics/bti476>
- Westfall, C., Flores-Mireles, A.L., Robinson, J.I., Lynch, A.J.L., Hultgren, S., Henderson, J.P., Levin, P.A., 2019. The widely used antimicrobial triclosan induces high levels of

antibiotic tolerance in vitro and reduces antibiotic efficacy up to 100-fold in vivo .

Antimicrob. Agents Chemother. 1–31. <https://doi.org/10.1128/aac.02312-18>

Who, 2014. ANTIMICROBIAL RESISTANCE Global Report on Surveillance 2014. World Heal. Organ.

Zwanenburg, G., Hoefsloot, H.C.J., Westerhuis, J.A., Jansen, J.J., Smilde, A.K., 2011.

ANOVA–principal component analysis and ANOVA–simultaneous component analysis:

A comparison. J. Chemom. <https://doi.org/10.1002/cem.1400>